Enzyme-Mediated Formation of Vesicles from DPPC−Dodecyl Maltoside Mixed Micelles

Brigitte Carion-Taravella,[‡] Sylviane Lesieur,[§] Michel Ollivon,[§] and Joël Chopineau *,[‡]

Contribution from the Laboratoire de Technologie Enzymatique, CNRS UPRES A 6022, 60205 Compiègne, France, and Equipe Physicochimie des Systèmes Polyphasés, CNRS URA 1218, 92296 Châtenay-Malabry, France

Received February 4, 1998

Abstract: An enzymatic procedure for liposome formation through micelle to vesicle transition is described. Amyloglucosidase hydrolysis of dodecyl-β-D-maltoside (DM) giving dodecyl-β-D-glucoside (DG) leads to dipalmitoylphosphatidylcholine (DPPC)-based vesicle formation from DPPC−DM mixed micelles. Starting from a 1.8 DM/DPPC molar ratio corresponding to mixed micelles, progressive hydrolysis of DM gives DPPC−DG−DM intermediate aggregates ending with DPPC−DG vesicles upon reaction completion. Initial steps of the process corresponding to the exit of the micellar domain were followed by turbidimetry measurements. Next, the reaction progress was investigated by RP-HPLC, HPLC-GEC, and cryofracture electron microscopy. A constant reaction rate is observed in the micellar domain, while the increase of the lamellae proportion considerably decreases the enzyme catalytic activity. Finally, the enzymatic hydrolysis is significally slowed when closed vesicles are formed. Enzymatic activity is dependent on DM availability in the bulk phase and of the DM/DPPC molar ratio in the aggregates. The presence of mixed micelles or lamellar sheets considerably modulates DM monomer concentration in the aqueous phase. The liposomes formed by the enzymatic process are spherical, unilamellar, and heterogeneous in size with a mean diameter ranging from 10 to 80 nm.

Introduction

The consequences of cell microstructuration on enzyme functions and the need of geometrically restricted systems to reproduce the complexity and the diversity of cell organization led to an approach which used biomimetic environments called microheterogeneous systems obtained from water/surfactant/organic solvent mixtures.[1,2] The study of relationships between enzymes and microorganized media was envisaged in microstructured systems with the same physicochemical features as the structures found at the cellular level.[3,4] Indeed, ternary mixtures composed of surfactant, water, and organic solvent provide a variety of colloidal organizations capable of self-evolution through the dynamic interactions of their components with an enzyme.[5] Such systems also permit following enzymatic reactions in restricted environments,[6] wherein the enzyme is responsible for environmental changes which in turn modulate enzyme catalytic activity. Self-replicating systems, based on dynamic interactions between amphiphilic aggregates (micelles, reversed micelles, vesicles) and enzymes, have been developed in relationship with autopoiesis.[7,8]

However, in these studies, the chemical nature of the product(s) and the phases formed are far from reproducing cell conditions. Indeed, the rationale of such work would be greater if natural molecules and systems of biological relevance such as phospholipids and liposomes were used instead of organic solvent−water based mesophases. In this respect, phospholipid(s)−surfactant(s) mixtures form numerous types of aggregates in water depending on their relative proportions.[9] Removal of the solubilizing surfactant (detergent) from mixed micelles results in vesicle formation through the so-called micelle−vesicle transition.[10−18] The latter is involved in many processes of liposome preparation[10−12,14,15,19] and in the extraction and the reconstitution of biomembrane proteins.[20−22]

In a preliminary work,[23] the possibility of liposome formation through enzymatic processes was described. Two distinct

[‡] To whom correspondence should be addressed. E-mail: joel.chopineau@utc.fr.

[§] Laboratoire de Technologie Enzymatique.

[‡] Equipe Physicochimie des Systèmes Polyphasés.

(1) Martinek, K.; Levashov, A. V.; Khmelnitsky, Y. L.; Klyachko, N. L.; Berezin, I. V. *Science* **1982**, *218*, 889−891.

(2) Luisi, P. L. *Angew. Chem., Int. Ed. Engl.* **1985**, *24*, 439−450.

(3) Klyachko, N. L.; Levashov, A. V.; Pshezhetsky, A. V.; Bogdanova, N. G.; Berezin, I. V.; Martinek, K. *Eur. J. Biochem.* **1986**, *161*, 149−154.

(4) Luisi, P. L.; Giomini, M.; Pileni, M. P.; Robinson, B. H. *Biochim. Biophys. Acta* **1988**, *947*, 209−246.

(5) Chopineau, J.; Thomas, D.; Legoy, M. D. *Eur. J. Biochem.* **1989**, *183*, 459−463.

(6) Chopineau, J.; Ollivon, M.; Thomas, D.; Legoy, M. D. *Pure Appl. Chem.* **1992**, *64*, 1757−1763.

(7) Bachmann, P. A.; Walde, P.; Luisi, P. L.; Lang, J. *J. Am. Chem. Soc.* **1991**, *113*, 8204−8209.

(8) Schmidli, P. K.; Schurtenberger, P.; Luisi, P. L. *J. Am. Chem. Soc.* **1991**, *113*, 8127−8130.

(9) Israelachvili, J. N. In *Physics of amphiphiles: micelles, vesicles, microemulsions*; Degiorgio, V., Corti, M. Eds.; North-Holland Physics Publishing-Elsevier: Amsterdam, 1985; 24−58.

(10) Lichtenberg, D. *CRC Handbook of Chemistry and Physics*; CRC Press: Boca Raton, 1996; pp 199−218.

(11) Paternostre, M.-T.; Roux, M.; Rigaud, J.-L. *Biochemistry* **1988**, *27*, 2668−2677.

(12) Ollivon, M.; Eidelman, O.; Blumenthal, R.; Walter, A. *Biochemistry* **1988**, *27*, 1695−1703.

(13) Ueno, M. *Biochemistry* **1989**, *28*, 5631−5634.

(14) Da Graça Miguel, M.; Eidelman, O.; Ollivon, M.; Walter, A. *Biochemistry* **1989**, *28*, 8921−8928.

(15) Vinson, P. K.; Talmon, Y.; Walter, A. *Biophys. J.* **1989**, *56*, 669−681.

(16) Kameyama, K.; Takagi, T. *J. Colloid Interface Sci.* **1991**, *146*, 512−524.

(17) Beugin, S.; Grabielle-Madelmont, C.; Paternostre, M.; Ollivon, M.; Lesieur, S. *Prog. Colloid Polym. Sci.* **1995**, *98*, 206−211.

(18) Paternostre, M.; Meyer, O.; Grabielle-Madelmont, C.; Lesieur, S.; Ghanam, M.; Ollivon, M. *Biophys. J.* **1995**, *69*, 2476−2488.

(19) Almog, S.; Litman, B. J.; Wachtel, E. J.; Barenholz, Y.; Ben-Shaul, A.; Lichtenberg, D. *Biochemistry* **1990**, *29*, 4582−4592.

10.1021/ja980400a CCC: $15.00 © 1998 American Chemical Society
Published on Web 10/06/1998

enzymatic preparations of liposomes from micelles or open structures composed of classical amphiphilic compounds have been proposed. One example was based on our knowledge concerning DPPC−alkylglucosides micelle-to-vesicle transition, while the second involved cholesterol-PEG derivatives as solubilizing lipids. For the first system, dipalmitoylphosphatidylcholine (DPPC)-based vesicles were obtained from DPPC-dodecyl-β-D-maltoside (DM) mixed micelles. Only the initial starting mixed micelles and the final liposome suspension were characterized. The intermediate states of aggregation and the phases encountered during the process were not approached. Moreover, the influence of enzyme kinetics on the structural transformation of the lipid assemblies and vice versa were not elucidated. The consecutive DM hydrolysis by amyloglucosidase and β-D-glucosidase was initially envisaged to remove the surfactant entirely, forming two molecules of glucose and one of dodecanol. In fact, DM hydrolysis by amyloglucosidase alone leaves an interesting bilayer-compatible surfactant, dodecyl-β-D-glucoside (DG), appearing to play the main role in the micelle−vesicle transition process. This is supported by the determination of the phase sequences and their boundaries in the DPPC−DG−DM ternary system upon DPPC and DPPC−DG vesicle solubilization by DM.[24]

In this work, DPPC−DG vesicles formation induced by amyloglucosidase hydrolysis of DM from DPPC−DM mixed-micelle solutions was considered in the framework of the DPPC−DG−DM ternary phase diagram. Amyloglucosidase kinetics toward DM was studied with and without the presence of lipid. The first steps of the enzyme-mediated vesicle formation were monitored by turbidimetry. The closure of the bilayered aggregates was examined by high performance gel exclusion chromatography (HPLC-GEC) and cryofracture electron microscopy.

Experimental Section

Chemicals. Amyloglucosidase (1,4-α-D-glucan glucohydrolase EC 3.2.1.3) from *Aspergillus niger*, DL-α-dipalmitoylphosphatidylcholine (DPPC, purity 99%), *N*-dodecyl-β-D-glucopyranoside (DG, purity 98%), *N*-dodecyl-β-D-maltoside (DM, purity 98%) and *p*-nitrophenyl-α-D-glucopyranoside (*p*-NPG, purity 99%) were purchased from Sigma. These products were used without further purification. All of the experiments were carried out using 145 mM NaCl, 10 mM HEPES (*N*-[2-hydroxyethyl]piperazine-*N*′-[2-ethanesulfonic acid]) buffer, pH 7.4.

Enzymatic Activity Measurements at 37 °C. The amyloglucosidase extract is composed of two isoenzymes, G1 and G2. Their molecular weights as determined by SDS-Page electrophoresis (Phast-System, Pharmacia) were equal to 75 000 and 105 000 g mol^{-1} respectively, in accordance with literature data (MW_{G1} = 82 000−100 000 g mol^{-1} and MW_{G2} = 110 000−112 000 g mol^{-1}).[25,26]

Enzyme quantities were determined by weight and by measuring the absorbance at 280 nm using a molar extinction coefficient of 1.53 × 10^5 M^{-1} cm^{-1} (ϵ_{280} = 1.37 × 10^5 M^{-1} cm^{-1} for amyloglucosidase G1).[27]

Spectrophotometric Measurements. Amyloglucosidase activity in buffer was measured by spectrophotometric analysis of hydrolysis of *p*-NPG. In a typical experiment, 1 mL of the aryl-α-D-glucoside solution (3 mM) in a citrate−phosphate buffer (50 mM, pH 5.2) was placed inside a spectrophotometer thermostated cuvette and 10 μL of an enzyme stock solution was added. The *p*-nitrophenol liberated was continuously measured by recording optical density at 380 nm (ϵ_{380} = 1227 M^{-1} cm^{-1} for *p*-nitrophenol under these experimental conditions).

Reverse Phase High-Performance Liquid Chromatography (RP-HPLC). Amyloglucosidase activity toward DM was studied following the surfactant disappearance using a C18 μbondapack column (3.9 × 300 mm) connected to an HPLC apparatus equipped with a 410 refractometer (Millipore Waters). Prior to use, the column was equilibrated with a 2.5 mM DM aqueous solution. In a typical experiment, the reaction was started by the addition of 50 μL of an enzyme stock solution to the lipid and/or surfactant mixture (6−7 mL) previously placed inside a 10-mL vial. A Gilson 232−401 automatic sample processor and injector were used for sampling. For each measurement, aliquots of (50−100 μL) were withdrawn and either added to an acetonitrile/water (50% v/v) mixture containing hexanol (50 mM) as internal standard or not. The column was loaded with 20 μL samples. The eluant (acetonitrile/water 50% v/v) was flushed at 1 mL/min. Under these conditions, the alkylglucosides DM and DG were eluted in two distinct peaks. Reaction rates were calculated from the kinetic curves plotting DM concentration as a function of time. One unit corresponds to the enzymatic activity that will hydrolyze 1 μmol of substrate per minute under these conditions.

Monitoring of Vesicle Formation by the Enzymatic Process. Mixed Aggregates Preparation. DPPC−DM mixed aggregates were prepared from a dried lipid−surfactant film formed from a mixed surfactant(s)−lipid chloroform solution by removing the organic solvent under a nitrogen stream followed by 12 h drying under vacuum. Mixed micelles were obtained by adding buffer and gentle mixing, while DPPC and DPPC−DG small unilamellar vesicles (SUV) were prepared by ultrasonic irradiation, according to a procedure already described.[28] For encapsulation experiments, dry DPPC or DPPC−DG films were hydrated by using 10 mM HEPES, pH 7.4 buffer containing 1 mM calcein and 140 mM NaCl to maintain the same osmolarity as that of the 145 mM NaCl buffer used for the gel exclusion chromatography analysis.

Turbidity Measurements. In a typical experiment, the mixed micelles solution was placed in a 3 mL optical quartz cell (Hellma, France) thermostated at 37 °C, equipped with a paddle stirrer that did not interfere with the light path. To start the reaction, 15 μL of amyloglucosidase solution was added to 1.5 mL of DPPC−DM mixed micelles (0.40 μM ≤ final enzyme concentration ≤ 0.90 μM). Turbidity at 400 nm was recorded using a Perkin-Elmer Lambda 2 double-beam spectrophotometer.

Characterization of the Aggregates. High Performance Gel Exclusion Chromatography (HPLC-GEC). Separation of nonentrapped calcein from calcein encapsulated in the vesicles was performed by using HPLC TSK-G6000 PW and TSK-G4000 PW 30 × 0.75 cm columns (Toyo Soda) connected in series.[29] The HPLC apparatus was equipped with a Hitachi pump (model L-6000) and a precision injection valve (Rheodyne). The eluant was aqueous buffer devoid of calcein. Prior to analysis, the columns were saturated with DPPC−DG vesicles prepared without calcein. Sample loading was 200 μL, and eluant flow rate was 1.0 mL/min. Elution was monitored on line by using a circulating quartz cell (Hellma) and placed in a spectrofluorimeter SPEX (FL1T11). The fluorescence emission intensity of calcein at 419 nm (excitation wavelength, 367 nm) and 90° light-scattering intensity of particles (incident wavelength, 367 nm) were simultaneously recorded as a function of elution time. The effective exclusion volume (V_0 = 9.7 mL) of the two columns in series was determined according to the

(20) Helenius, A.; Simons, K. *Biochim. Biophys. Acta* **1975**, *415*, 29−79.
(21) Rabilloud, T.; Fath, S.; Baur, E.; Egly, J.-M.; Relevant, O. *Biofutur* **1993**, 126.
(22) Rigaud, J.; Pitard, B.; Levy, D. *Biochim. Biophys. Acta* **1995**, *1231*, 223−246.
(23) Chopineau, J.; Lesieur, S.; Ollivon, M. *J. Am. Chem. Soc.* **1994**, *116*, 11582−11583.
(24) Carion-Taravella, B.; Chopineau, J.; Ollivon, M.; Lesieur, S. *Langmuir*, **1988**, *14*, 3767−3777.
(25) Swensson, B.; Larsen, K.; Svendsen, I.; Boel, E. *Carlsberg Res. Commun.* **1983**, *48*, 529−544.
(26) Pazur, J. H.; Knull, H. R.; Cepure, A. *Carbohyd. Res.* **1971**, *20*, 83−96.
(27) Clarke, A. J.; Swensson, B. *Carlsberg Res. Commun.* **1984**, *49*, 111−121.
(28) Lesieur, S.; Grabielle-Madelmont, C.; Paternostre, M.-T.; Moreau, J. M.; Handjani-Villa, R. M.; Ollivon, M. *Chem. Phys. Lipids* **1990**, *56*, 109−121.
(29) Andrieux, K.; Lesieur, S.; Ollivon, M.; Grabielle-Madelmont, C. *J. Chromatogr. B* **1998**, *706*, 141−147.

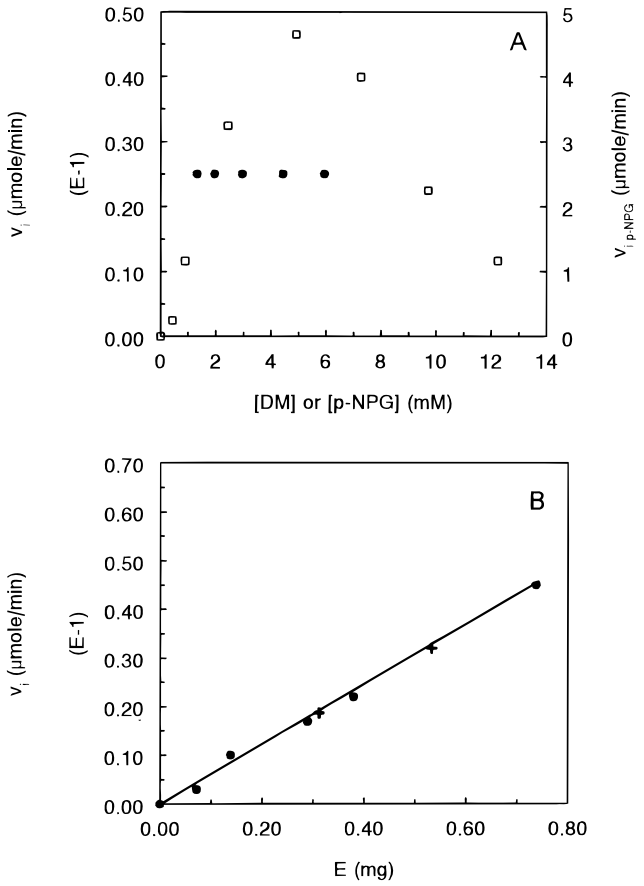

Figure 1. (A) Variations of the initial reaction rates versus substrate concentration for DM (v_i, (●) or *p*-NPG ($v_{i\ p-NPG}$, (□) hydrolysis at a constant amyloglucosidase concentration of 0.6 μM or 5.3 μM, respectively. (B) Variation of initial reaction rate of DM hydrolysis as a function of amyloglucosidase concentration from (●) pure DM micelles ($[DM]_0 = 4.0$ mM) or from (+) mixed DPPC−DM micelles ($[DM]_0 = 9.0$ mM, [DPPC] = 4.5 mM).

elution of nonextruded multilamellar egg phosphatidylcholine/egg phosphatidic acid vesicles. The total volume ($V_t = 21.5$ mL) was given by elution of NaCl by using a 410 differential refractometer as detector (Millipore Waters).[30]

Cryofracture Electron Microscopy. Sample suspension (without cryoprotectant) was placed on a hollow gold−copper cup (Bal-Tec) with a centered shaft of 1 mm diameter. The preparation was placed on a sample holder and transferred to a quick-freeze apparatus. Freezing was obtained by projection of the sample against a highly cleaned copper block (Reichert and Jung) cooled by liquid helium (4 K) and maintained under vacuum. The specimen was fractured using a Balzers freeze-fracture apparatus at 133 K and under high vacuum (2×10^{-10} bar). The fractured sample is replicated by platin/carbon shadowing. The replica is washed with distilled water overnight and placed on a gold mesh grill. Electron micrographs were obtained with a transmission electron microscope (Leo EM912).

Results

Enzymatic Kinetic Studies. First, amyloglucosidase activity toward a hydrosoluble substrate, *p*-NPG, was examined. A non-Michaelis−Menten mechanism was observed with an inhibition by excess of substrate obtained above 5 mM of *p*-NPG (Figure 1A). A specific activity of 6 IU mg^{-1} was determined using a Linweaver−Burk plot $\{1/v_i = f(1/[p\text{-NPG}])\}$ between 0 and 4.6 mM of *p*-NPG. Similar inhibition effects were found for the hydrolysis of *p*-NPG and *p*-nitrophenyl-β-D-galactoside by a β-glucosidase and a β-galactosidase, respectively.[31,32] Second, the enzyme activity was checked on both DM and DG by thin-layer chromatography according to conditions previously described.[5] In both cases, no dodecanol was detected, indicating that DG is not hydrolyzed. This confirms the amyloglucosidase stereospecificity toward the α-glucosidic bond of DM.

Kinetics of DM hydrolysis by amyloglucosidase were examined on pure surfactant micelles. The disappearance of DM was followed by RP-HPLC. The initial reaction rate (v_i) versus DM concentration is plotted in Figure 1A. For a given enzyme concentration, v_i is constant in the 1−6 mM DM concentration range. Moreover, a linear relationship between v_i and amyloglucosidase content is found and used to calculate a specific activity (Figure 1B). The specific activity was found to range from 0.04 to 0.06 IU mg^{-1} as a function of the enzyme batch and storage period. In the following, the specific activity was normalized to 0.06 IU mg^{-1} (Figure 1B). These results suggest that the amyloglucosidase recognizes the DM monomer as effective substrate. Accordingly, this behavior was demonstrated for another glucohydrolase, β-D-glucosidase, toward octyl-β-D-glucopyranoside (OG).[6] Unfortunately, due to both low critical micelle concentration (cmc) of DM (0.13 mM)[24] and the limit of refractive index detection (0.1 mM), hydrolysis experiments below DM cmc cannot be performed under these RP-HPLC conditions.

Amyloglucosidase activity toward DM in the presence of DPPC was studied for an initial DM/DPPC molar ratio equal to 1.8 which imposes the presence of isotropic mixed micelles solution.[24] During enzymatic reaction, DM removal was monitored by RP-HPLC. The variations of total DM concentration as a function of time ([DM](t)) are illustrated by Figure 2A at different enzyme and/or lipid contents. The velocity dependence was obtained by plotting the d([DM](*t*))/d*t* as a function of time (Figure 2B). Three regimes in reaction rate (corresponding to regions 1, 2, and 3 on parts B and C of Figure 2) can be identified as a function of time. In region 1, a constant amyloglucosidase initial activity of 0.06 IU mg^{-1} toward DM was found at both a given enzyme or DPPC content, this indicates that the initial rate of substrate hydrolysis only depends on the DM concentration. This value is identical to that obtained by hydrolysis from pure DM micelles which suggests that the presence of lipids does not affect the specific activity of the enzyme (Figure 1B). In region 2, the rate of the reaction is significantly affected and decreases rapidly to 0.01 IU mg^{-1}. Finally, in region 3, the reaction rate is very slow and close to null. In Figure 2C, from plotting the enzyme velocity as a function of the total DM/DPPC molar ratio, each regime change clearly appears at a constant total DM/DPPC molar ratio and does not depend on the DPPC or enzyme concentrations. In particular, the first regime change corresponds to a molar ratio of 0.7 (Figure 2C, arrow).

Vesicle Formation. The addition of amyloglucosidase to DPPC−DM mixed micelles leads to progressive production of DG as a replacement for DM. Consequently, during the enzymatic process, the system is constituted by aqueous DPPC−DG−DM evolving ternary mixtures. The technique consisting of recording the optical density (OD) of the sample as a function of surfactant concentration is widely used to follow morphological changes of the aggregates occurring during vesicle-to-micelle transition.[11,12,17,33−35] In this study, turbidimetry was applied to identify the first steps of the enzymatic process.

(30) Beugin-Deroo, S. Ph.D. Thesis, Université Paris VI, 1997.

(31) Gabelsberger, J.; Liebl, W.; Schleifer, K. H. *Appl. Microbiol. Biotechnol* **1993**, *40*, 44−52.

(32) Pulvin, S.; Friboulet, A.; Thomas, D. *Biochim. Biophys. Acta* **1990**, *1041*, 97−100.

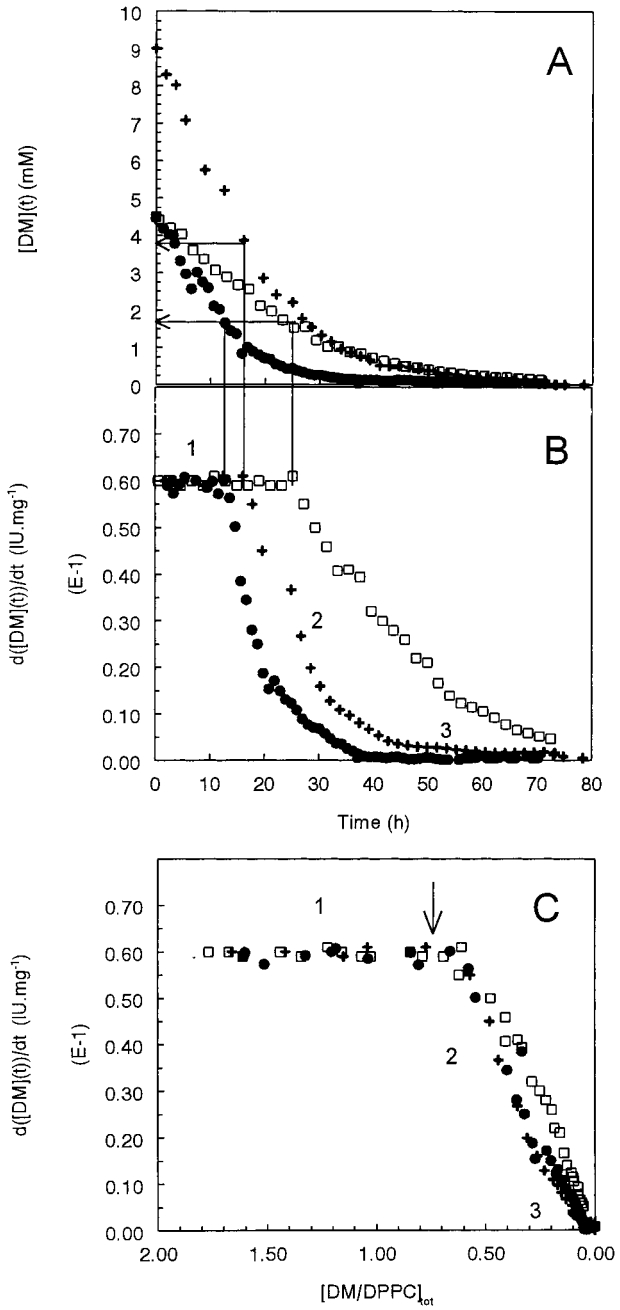

Figure 2. DM hydrolysis by amyloglucosidase starting from DPPC−DM mixed micelles. (A) Total DM concentration [DM](t) and (B) reaction rate d([DM](t))/dt evolutions as a function of time; (C) d([DM](t))/dt variation as a function of total DM/DPPC molar ratio. Respective enzyme (E) and DPPC concentrations are [E] = 1.2 μM, [DPPC] = 2.5 mM (●); [E] = 0.6 μM, [DPPC] = 2.5 mM (□) and [E] = 1.2 μM, [DPPC] = 5.0 mM (+). The d([DM](t))/dt values are related to enzyme content and expressed in IU mg^{-1}. Numbers 1, 2, and 3 indicate the different regimes of reaction rate. [DM] or [DM/DPPC]$_{tot}$ values at the rate changes from regime 1 to regime 2 are either given by the projection (solid lines) of breaks of the curves in (B) onto the corresponding curves in (A), or indicated by the arrow in (C).

Reactions were performed starting from DPPC−DM mixed-micelles solutions with a surfactant-to-lipid molar ratio of 1.8. In two series of experiments, the influence of both amyloglucosidase and DPPC concentrations was studied. Homothetic curves were obtained in both cases. They are illustrated for different enzyme concentrations in Figure 3. They present a similar complex shape depicting an uneven turbidity variation. The beginning of each curve is characterized by three break points noted as A, B, and C (Figure 3, inset), corresponding to drastic OD variations. The initial OD measurements revealed low values which are attributed to mixed micelles (up to point A), and the sharp increase which follows (from A to C) depicts changes in the morphology and/or interactions of the aggregates formed during the hydrolysis or is the result of phase-separation phenomena. The higher the enzyme concentration, the faster the different characteristic break points are reached. According to Figure 4, this increase in turbidity observed during the earlier steps of the enzymatic process and characterized by A, B, and C break points corresponds to regime 1 of the hydrolysis rate, that is, to a constant hydrolysis rate (Figure 2). Figure 4 easily allows the determination of the DM/DPPC total molar ratio corresponding to modifications of the reaction rate regime by the projection of the breaks of the rate curve d([DM](t))/dt vs t onto the [DM/DPPC]$_{tot}$ vs t curve. The ends of regimes 1 and 2 correspond to [DM/DPPC]$_{tot}$ equal to 0.7 and 0.3, respectively.

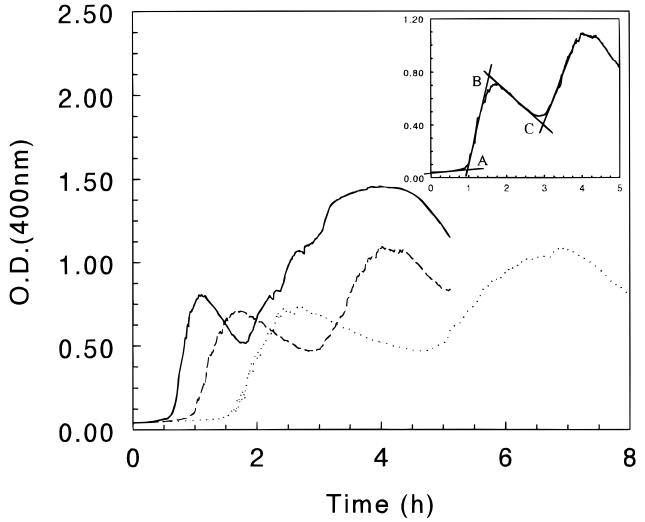

Figure 3. Variation of OD at 400 nm during DM hydrolysis by amyloglucosidase for different amyloglucosidase concentrations. The initial medium (t = 0) is composed of DPPC−DM mixed micelles. [E] = 0.40 μM (solid line), [E] = 0.60 μM (dashed line) and [E] = 0.90 μM (dotted line). [DPPC] = 1.48mM. Inset: A, B, and C denote the characteristic break points determined by the intercept of the tangents to the turbidity curves.

Two series of turbidity curves by varying DPPC and/or enzyme concentrations ([E] = 0.60 μM for 0.3 mM < [DPPC] < 3 mM; 0.3 < [E] < 1.0 μM for [DPPC] = 1.5 mM) were worked out in order to obtain DM concentrations at the characteristic turbidity points (A to C). The overall DM concentration ([DM](t)) at any time is calculated during the reaction using the following equation

$$[\mathrm{DM}](t) = [\mathrm{DM}]_0 - (\int v_{(t)}\,\mathrm{d}t)/V_{\mathrm{tot}} \qquad (1)$$

where [DM](t) equals the total DM concentration at time t (mM), $[\mathrm{DM}]_0$ equals the initial DM concentration (mM), $v_{(t)}$ equals the instantaneous reaction rate (μmole/min), t equals the time in minutes, and V_{tot} equals the total reaction volume (mL). Throughout the DPPC and DM concentration range corresponding to the turbidity break points, the specific activity of the

(33) Lichtenberg, D.; Robson, R. J.; Dennis, E. A. *Biochim. Biophys. Acta* **1983**, *737*, 285−304.
(34) Seras, M.; Edwards, K.; Almgren, M.; Carlson, G.; Ollivon, M.; Lesieur, S. *Langmuir* **1996**, *12*, 330−336.
(35) De La Maza, A.; Parra, J. L. *Biophys. J.* **1997**, *72*, 1668−1675.

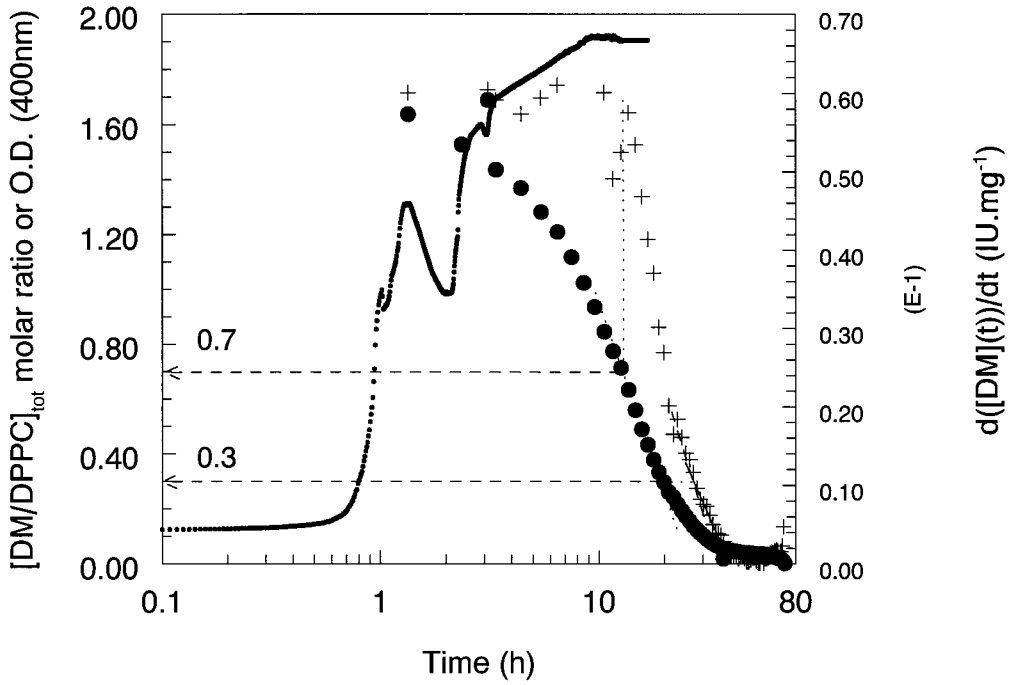

Figure 4. Variation of DM/DPPC total molar ratio (●), turbidity (•) and reaction rate d([DM](*t*))/d*t* (+) as a function of time (logarithm axis scaling); [E] = 0.6 μM, [DPPC] = 2.5 mM. The d([DM](*t*))/d*t* values are related to enzyme content and expressed in IU mg^{-1}. Characteristic DM/DPPC molar ratio values of 0.7 and 0.3 were determined by the projection of the breaks of the d([DM](t))/d*t* = *f*(*t*) curve onto ([DM/DPPC]$_{tot}$ = *f*(*t*) curve.

enzyme is constant and equal to 0.06 IU mg^{-1} (Figures 1B and 4). Equation 1 is simplified as follows

$$[\mathrm{DM}](t) = [\mathrm{DM}]_0 - 0.06\mathrm{E}t/V_{\mathrm{tot}} \qquad (2)$$

where E corresponds to the enzyme content (mg).

At each break point, A, B, and C, the total DM concentration ([DM](*t*)) was plotted versus the total DPPC concentration ([DPPC]) (data not shown).[18,33,36] The DPPC concentration in the aggregates is considered equal to the total DPPC content according to its very low critical aggregation concentration (5 $\times$ 10^{-10}M).[37] Linear relationships with correlation coefficients of 0.99 were found for each break point family depicted by the following equation

$$[\mathrm{DM}](t) = [\mathrm{DM}]_{\mathrm{bulk}} + [\mathrm{DM/DPPC}]_{\mathrm{agg}}\,[\mathrm{DPPC}] \qquad (3)$$

The concentration of DM molecules which are not associated with the lipid $[DM]_{bulk}$ is given by the extrapolation to zero of the total DPPC concentration, and the surfactant-to-lipid molar ratio in the aggregates $[DM/DPPC]_{agg}$ is determined from the slopes of the straight lines. Values of $[DM]_{bulk}$ and $[DM/DPPC]_{agg}$ at break points A, B, and C are summarized in Table 1, as well as the total DM-to-DPPC molar ratios $[DM/DPPC]_{tot}$. The $[DM]_{bulk}$ values, varying from 0.03 to 0.11 mM, agree with the cmc value of pure DM. Indeed, in the presence of DPPC, DM (given its amphiphilic character) partitions between lipidic assemblies and aqueous phase, and its concentration in the water phase should range from 0 to a maximum equal to the cmc of DM in the absence of lipid molecules (0.13 mM).[24]

The aggregates formed during the enzymatic process were characterized by HPLC-GEC in the presence of a water-soluble fluorescent probe, calcein, (Figure 5). Indeed, this technique is a useful tool to demonstrate vesicle-like aggregates and to detect their eventual closure by evaluating their ability to entrap and retain calcein initially present in the aqueous medium.[38] Three initial amyloglucosidase concentrations, 0.3 μM (Figure 5, curve a), 0.6 μM (Figure 5, curve b), and 1.2 μM (Figure 5, curve c), were examined at a total lipid concentration of 10 mM. Chromatography analysis was performed at 5 days enzymatic reaction. DM concentrations were determined by RP-HPLC, leading to calculated total DM/DPPC molar ratios in the analyzed particles of 1.35 (Figure 5, curve a), 1.04 (Figure 5, curve b), and 0.33 (Figure 5, curve c), respectively. Pure DPPC vesicles prepared by ultrasonic irradiation in the presence of calcein were used as a reference (Figure 5, curve d). For the three enzyme concentrations studied, fluorescence detection reveals a first peak with a maximum located between 14.5 and 16 mL, which is within the elution region of large particles, and a second split peak centered at 21 mL very close to the total elution volume of the columns (Figure 5A). The position of the first peak is superimposed on those obtained by 90° light-scattering detection and nearly coincides with the elution profiles of the DPPC vesicles used as a standard (14 mL maximum

Table 1. Concentration of DM in the Aqueous Phase $[DM]_{bulk}$, Surfactant(s) Mixed Aggregate Compositions $[DM/DPPC]_{agg}$, and Total DM/DPPC Molar Ratio $[DM/DPPC]_{tot}$ at the Break Points of the Turbidity Curves Obtained upon Enzymatic Hydrolysis of DM from DPPC−DM Mixed Micelles[a]

break point	$[DM]_{bulk}$[b] (mM)	$[DM/DPPC]_{agg}$[b]	$[DM/DPPC]_{tot}$
A	0.05 ± 0.03	1.66 ± 0.03	1.71 ± 0.03
B	0.11 ± 0.06	1.46 ± 0.07	1.54 ± 0.08
C	0.03 ± 0.02	1.40 ± 0.07	1.43 ± 0.07

[a] Calculations of total DM concentrations were done according to eq 2. [b] Partition parameters were obtained from linear regression analysis according to eq 3.

(36) Levy, D.; Gulik, A.; Seigneuret, M.; Rigaud, J. *Biochemistry* **1990**, *29*, 9480−9488.

(37) Marsh, D. *Handbook of Lipid Bilayers*; CRC Press: Boca Raton, 1990; p 276.

(38) Lesieur, S.; Grabielle-Madelmont, C.; Paternostre, M.; Ollivon, M. *Chem. Phys. Lipids* **1993**, *64*, 57−82.

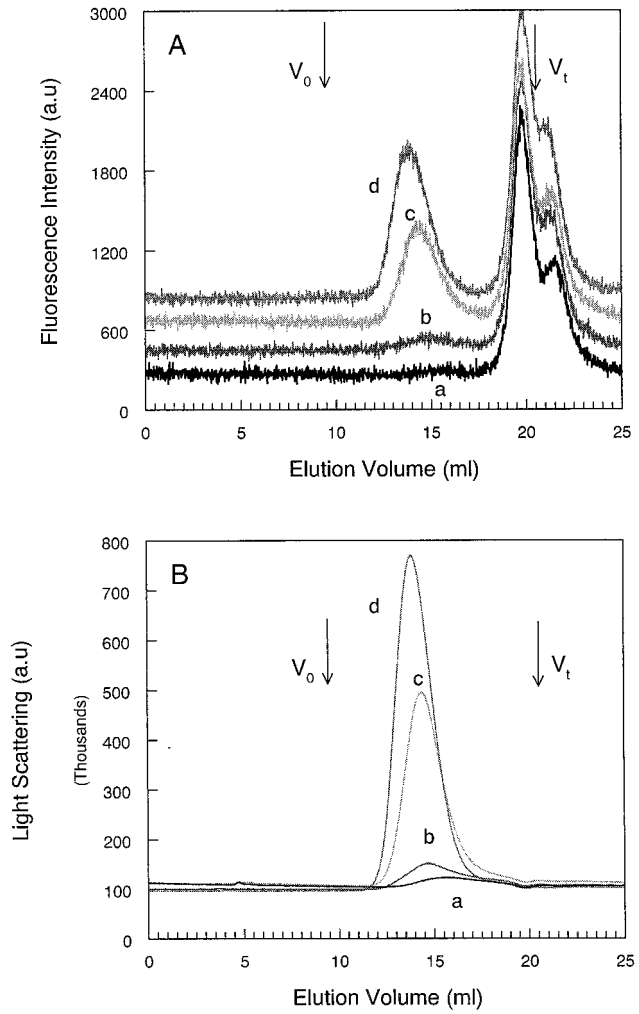

Figure 5. Gel exclusion chromatography profile of aggregates formed during the enzymatic process for a total DPPC concentration of 5 mM (initial [DM/DPPC] = 1.8) and in the presence of 1 mM calcein. [E] = 0.3 μM (a), [E] = 0.6 μM (b), and [E] = 1.2 μM (c). Chromatography analysis was made at 5 days of the enzymatic reaction. Total DM concentrations of the samples are 1.67 mM (a), 5.2 mM (b), and 6.7 mM (c) from RP-HPLC. Curve d corresponds to sonicated pure DPPC vesicles ([DPPC] = 10 mM). (A) Fluorescence (excitation at 367 nm; emission at 419 nm), (B) 90° light scattering at 367-nm on-line detection. Flow rate, 1 mL/min. Void (V_0) and total (V_t) volumes of the columns are indicated by arrows. The chromatograms in A are shifted along the *y*-axis by adding an arbitrary constant to the base line.

elution volume) (Figure 5B). This peak thus corresponds to closed vesicles containing calcein. The second peak is superimposed with the chromatogram of a 1 mM calcein solution and is ascribable to the nonencapsulated probe molecules. The intensity of the vesicle elution peaks detected by both fluorescence and light scattering increases with increasing amyloglucosidase content, indicating that the higher the enzyme concentration, the higher the amount of closed aggregates formed after a 5-day reaction time.

A cryofracture electron microscopy analysis was made to visualize the enzymatically formed aggregates. Following complete reaction, closed vesicles heterogeneous in size with a diameter ranging from 10 to 80 nm are observed (Figure 6A). They are comparable with standard vesicles obtained by ultrasonication of DPPC−DG−DM mixture (1:1.7:0.1 molar ratio) which are unilamellar and homogeneous in size (mean diameter of 50 nm) (Figure 6B) and ref 24.

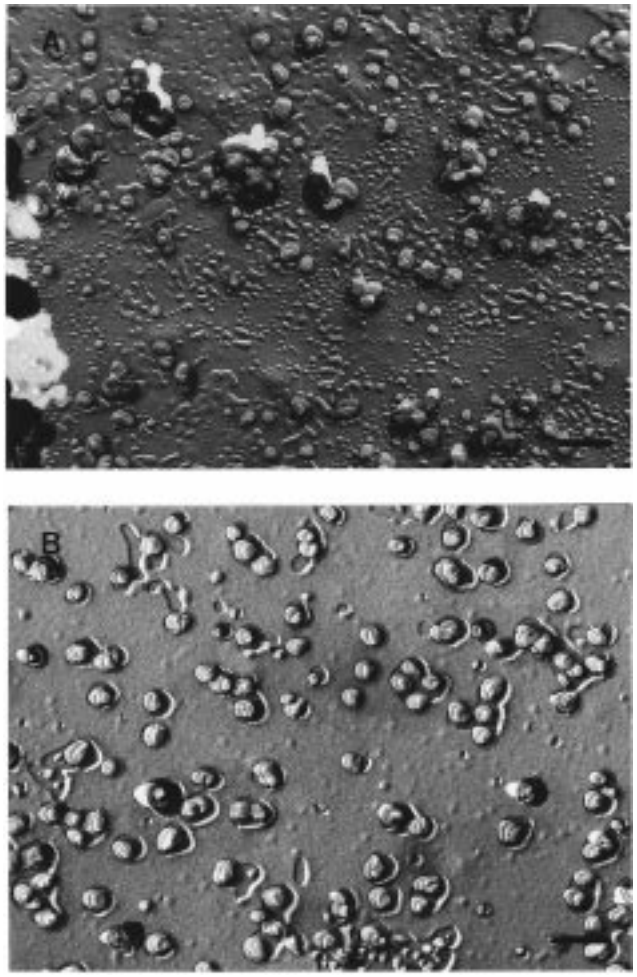

Figure 6. Freeze-fracture electron microscopy of (A) DPPC−DG vesicles obtained at 5 days of enzymatic reaction from DPPC−DM mixed micelles ([DPPC] = 5mM, initial DM/DPPC molar ratio equal to 1.8, [E] = 2.4 μM, T = 37 °C) and (B) DPPC−DG−DM (1:1.7:0.1 molar ratio) vesicles obtained by ultrasonic irradiation ([DPPC] = 10 mM). A constant temperature of 37 °C was maintained until freezing. Bar = 130 nm.

Discussion

From the results presented in this work, it clearly appears that the enzyme kinetics in this process are connected to the lipid−surfactant aggregation state. To clarify the interactions between amyloglucosidase reactivity and the supramolecular structures, phase behavior of the system along the enzymatic pathway from mixed micelles to vesicles was examined. The pseudoternary DPPC−DG−DM partial phase diagram at 37 °C was established recently by turbidimetry, performed along the solubilization process of DPPC and DPPC−DG vesicles by DM, and the structures of the phases confirmed by small-angle X-ray scattering.[24] A schematic representation of it is reproduced in Figure 7. With the enrichment in DG (or the decrease of DM), four main phase domains are crossed, a micellar solution, a biphasic domain constituted of micelles separated from a water-rich upper phase (clouding phenomenon), a coexistence domain including micelles and lamellar assemblies, and a vesicle dispersion.

In the diagram of Figure 7, enzymatic pathways are very close to straight lines joining binary DPPC−DM and DPPC−DG mixtures of the same molar ratio. This is based on the isomolar stoichiometry of DM hydrolysis into DG by amyloglucosidase and on the comparable solubilities of both surfactants in the

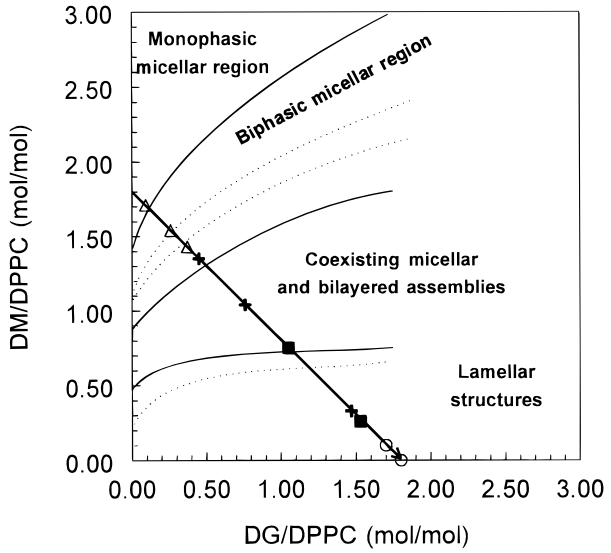

Figure 7. Partial pseudoternary DPPC−DG−DM phase diagram in excess buffer at 37 °C from ref 24. In such a plot (DM/DPPC as a function of DG/DPPC molar ratio in the aggregates), the axes correspond to the binary DPPC−DM and DPPC−DG systems, and excess water is implied and not represented. The solid lines delimit the main phase domains and the dotted lines indicate secondary aggregation state transitions. The arrow indicates the enzymatic reaction pathway on which are reported the compositions corresponding to the turbidity break points (△), amyloglucosidase kinetic analysis (■), samples examined by either HPLC−GEC (+) or cryofracture electron microscopy (○).

buffer used (cmc = 0.13 mM for DM and cmc = 0.16 mM for DG at 37 °C).[24] According to the very low solubility of both surfactants in the aqueous medium, their bulk concentrations are negligible. This is partly demonstrated by the $[DM]_{bulk}$ values in Table 1. Consequently, the total DM-to-DPPC or DG-to-DPPC molar ratios ($[DM/DPPC]_{tot}$ or $[DG/DPPC]_{tot}$, respectively) can be considered to be close to the molar ratios in the mixed aggregates ($[DM/DPPC]_{agg}$ or $[DG/DPPC]_{agg}$).

In this study, the experiments were performed along the line corresponding to a 1.8 total surfactant-to-lipid molar ratio and which is materialized by the arrow in Figure 7. The identification of the different aggregation steps involved in the enzymatic process was investigated by using four techniques, RP-HPLC (Figure 7, ■ symbol), turbidity measurements (Figure 7, △ symbol), HPLC-GEC (Figure 7, + symbol), and electron microscopy (Figure 7, ○ symbol).

Three regimes of reaction rates are observed as a function of the enzymatic progress (Figures 2 and 4). In the 1.8−0.7 DM/DPPC molar ratios range, the reaction rate is constant. The evolution of the aggregates in this region was studied by turbidimetry. Three main characteristic events are identified by break points A, B, and C (Figure 3). The corresponding compositions (Table 1) are reported on the enzymatic line in Figure 7 (△ symbol). These events are located in the micellar domain of the phase diagram. Point A coincides with the boundary between the micellar solution and the biphasic region (micelles separated from a water-rich subphase). In the biphasic region, both points B and C concur with macroscopic phase separations of mixed micelles from the aqueous phase (clouding phenomenon). The correspondence of the turbidity events with the micellar state transitions confort the use of eq 2. As a consequence, in this region, turbidity measurements can be used to determine the reaction progress and aggregate composition, providing enzyme specific activity is known. Beyond point C, turbidity curves fluctuate around high OD values, and no significant events, which would have been correlated, can be observed.

To circumvent the above-mentioned limitation, the aggregates formed upon amyloglugosidase hydrolysis were characterized by HPLC-GEC and electron microscopy. The velocity of the enzyme is progressively decreasing from 0.06 to 0.01 IU mg^{-1} in the 0.7−0.3 DM/DPPC molar ratio range (regime 2, Figures 2 and 4) and from 0.01 to nearly 0 IU mg^{-1} for DM/DPPC molar ratios below 0.3 (regimes 3, Figures 2 and 4). This concentration range coincides with the appearance of lamellar structures in coexistence with micelles (Figure 7, ■ symbol), that is, the higher the proportion of lamellar phase, the slower the reaction rate. Finally, when only lamellar bilayers subsist, the reaction is significantly slowed. Samples examined at the same time for different enzyme concentrations by HPLC-GEC move along the enzymatic pathway in the pure lamellar domain of the phase diagram. The molar ratios corresponding to the GEC samples are reported in Figure 7 (+ symbol). As the enzymatic reaction progresses, the increase in the lamellar structure proportion is accompanied by an increase in the number of large aggregates capable of retaining calcein (Figure 5A). These results indicate that the enzymatic kinetic is altered by the evolution of bilayers toward vesicle formation. This is supported by a very low reaction rate beyond the DM/DPPC molar ratio of 0.3 when the system is mainly composed of vesicles (Figure 5A). The electron micrography of the aggregates obtained at the end of the enzymatic reaction (Figure 6A) confirms the presence of closed vesicles within the region in which the amyloglucosidase velocity is quite reduced to zero (Figure 7, ○ symbol).

A possible explanation for the decrease and finally the annulment of the amyloglucosidase velocity as the hydrolysis of DM progresses may be the progressive enzyme encapsulation inside the vesicles. However, the internal volume of vesicles formed by this process calculated as a function of mean diameter (10−80 nm) and total lipid concentration (10 mM) represents only around 1% of the total dispersion volume, making this hypothesis unlikely. A second more conceivable suggestion for the slowing down of the reaction rate is that the DM availability may be reduced by the occurrence of bilayered structures to the detriment of micellar ones which may influence the DM migration from the aggregates toward the aqueous continuum. In favor of this hypothesis, kinetics studies have shown that the exchange of surfactant molecules between micelles and bulk phase and the intermicellar exchange of monomers are indeed very fast in the case of polyoxyethylene or sugar headgroup-based surfactants.[39−41] In contrast, in the presence of lamellar structures such as liposomes, the surfactant migration rate is significantly limited by slow translational diffusion through the lipid bilayer.[42,43] This limitation can be related to the freedom of movement of the surfactant molecule which is reduced from a 3-dimensional one in the micelle solution to a 2-dimensional one in the lamellar assemblies.[44]

(39) Malliaris, A.; Lang, J.; Sturn, J.; Zana, R. *J. Phys. Chem.* **1987**, *91*, 1475−1481.
(40) Frindi, M.; Michels, B.; Zana, R. *J. Phys. Chem.* **1992**, *96*, 6095−6102.
(41) Frindi, M.; Michels, B.; Zana, R. *J. Phys. Chem.* **1992**, *96*, 8137−8141.
(42) Annesini, M. C.; Di Giulio, A.; Di Marzio, L.; Finazzi-Agro, A.; Mossa, G. *J. Liposome Res.* **1992**, *2*, 455−467.
(43) Annesini, M. C.; Di Giorgio, L.; Di Marzio, L.; Finazzi-Agro, A.; Serafino, A. L.; Mossa, G. *J. Liposome Res.* **1994**, *3*, 639−648.
(44) Small, M. S. In *The Physical Chemistry of Lipids: From Alkanes to Phospholipids*; Hanahan, D. J., Ed.; Plenum Press: New York, 1986; pp 43−83.

Another factor influencing DM avaibility is its partioning between the lipid aggregates and the aqueous phase upon the enzymatic reaction. Indeed, it has been shown that the monomeric detergent concentration in the bulk phase increases throughout the vesicle-to-mixed micelle transition,[13,18,19,45] the ultimate stage of the solubilization process being characterized by mixed cmc values very close to the cmc of the pure surfactant.[12,18] The reversibility of the vesicle-to-micelle transition implies that, conversely, the surfactant content in the bulk phase progressively decreases with vesicle formation. This was verified for the PC−DM system.[35] Under such circumstances, DM hydrolysis by amyloglucosidase (the rate of which is proportional to the DM bulk concentration) would be considerably reduced as the vesicle formation progresses.

The change of the amyloglucosidase reaction rate as the reaction progresses from mixed micelles to lamellar sheets is also consistent with two relevant enzymatic studies. The first one concerns the study of the glucose oxidase catalysis in a micellar environment.[46] It was shown that all of the rate constants involved in the enzyme kinetics are unaffected by the presence of surfactant micelles. The second one is the β-D-glucosidase activity study toward OG micelles (up to 20% OG).[5] The authors have shown that in the presence of pure or mixed micelles, the enzyme activity is limited by the availability of the detergent in the aqueous continuum and the reaction rate is constant. Conversely, the formation of an OG/octanol/water lamellar phase from concentrated OG micelles upon the β-D-glucosidase reaction shows that the existence of lamellar sheets considerably decreases the reaction rate.[5,6]

In conclusion, these results together demonstrate that it is possible to move inside a ternary phase diagram using a specific enzyme converting one of the mixture components. Starting from the region of mixed micelles or similar "open" structures, the removal of the surface active agent through the enzymatic polar headgroup hydrolysis allows the system to evolve toward vesicle formation. Enzyme-induced transformation of non-vesicle aggregates into liposomes represents an alternative method for encapsulation of labile substances and, from a biochemical point of view, provides an insight into how enzymes may mediate structural transitions in biomembranes.

Acknowledgment. We are grateful to J-P. Lechaire and G. Frebourg. (Centre Inter-universitaire de Microscopie Electronique CNRS UPR 9042, Paris) for electron microscopy experiments.

JA980400A

(45) Rigaud, J.-L.; Paternostre, M.-T.; Bluzat, A. *Biochemistry* **1988**, *27*, 2677−2688.

(46) Deshaies, C.; Chopineau, J.; Moiroux, J.; Bourdillon, C. *J. Phys. Chem.* **1996**, *100*, 5063−5069.